

Bladder Accumulated Dose in Image-Guided High-Dose-Rate Brachytherapy for Locally Advanced Cervical Cancer and its Relation to Urinary Toxicity

Roja Zakariaee ^{a,b}, Ghassan Hamarneh ^c, Colin J Brown ^c, Marc Gaudet ^d, Christina Aquino-Parsons ^b, Ingrid Spadinger ^b

^a Department of Physics and Astronomy, University of British Columbia, Vancouver, BC, Canada

^b British Columbia Cancer Agency, Vancouver Centre, Vancouver, BC, Canada

^c Medical Image Analysis Lab, School of Computing Science, Simon Fraser University, Burnaby, BC, Canada

^d Division of Radiation Oncology, The Ottawa Hospital, Ottawa, ON, Canada

Purpose

The purpose of this study was to estimate locally accumulated dose to the bladder in multi-fraction high-dose-rate (HDR) image-guided intracavitary brachytherapy (IG-ICBT) for cervical cancer, and study the locally-accumulated dose parameters as predictors of late urinary toxicity.

Materials and Methods

A retrospective study of 60 cervical cancer patients who received five HDR IG-ICBT sessions was performed. The bladder outer and inner surfaces were segmented for all sessions and a bladder-wall contour point-set was created in MATLAB. The bladder-wall point-sets for each patient were registered using a deformable point-set registration toolbox called coherent point drift (CPD), and the fraction doses were accumulated. Various dosimetric and volumetric parameters were calculated using the registered doses, including rD_{ncm^3} (minimum dose to the most exposed $n\text{-cm}^3$ volume of bladder wall), rV_{mGy} (wall volume receiving at least m Gy), and $rEQD2_{ncm^3}$ (minimum equivalent biologically weighted dose to the most exposed $n\text{-cm}^3$ of bladder wall), where $n = 1/2/5/10$ and $m = 3/5/10$. Minimum dose to contiguous 1 and 2 cm^3 hot-spot volumes was also calculated. The unregistered dose volume histogram (DVH)-summed equivalent of rD_{ncm^3} and $rEQD2_{ncm^3}$ parameters (i.e. sD_{ncm^3} and $sEQD2_{ncm^3}$) were determined for comparison. Late urinary toxicity was assessed using the LENT-SOMA scale, with toxicity Grade 0-1 categorized as Controls and Grade 2-4 as Cases. A two-sample t-test was used to identify the differences between the means of Control and Case groups for all parameters. A binomial logistic regression was also performed between the registered dose parameters and toxicity grouping.

Results

Seventeen patients were in the Case and 43 patients in the Control group. Contiguous rD_{ncm^3} values were on average 16 and 18% smaller than sD_{ncm^3} parameters for 1 and 2 cm^3 volumes, respectively. Contiguous $rEQD2_{ncm^3}$ values were on average 26 and 27% smaller than $sEQD2_{ncm^3}$ parameters. The only statistically significant finding for Case versus Control based on both methods of analysis was observed for rV_{3Gy} ($p=0.02$).

Conclusions

DVH-summed parameters based on unregistered structure volumes overestimated the bladder dose in our patients, particularly when contiguous high dose volumes were considered. The bladder-wall volume receiving at least 3 Gy of accumulated dose may be a parameter of interest in further investigations of Grade 2+ urinary toxicity.

Keywords: Brachytherapy, Bladder, Toxicity, Accumulated Dose, Deformable Registration, Cervical Cancer

Submitted to *Phys. Med. Biol.* on March 16, 2016

Revision submitted on August 22, 2016

1 Introduction

2 Radiation therapy has long been a standard treatment for locally advanced carcinoma of the cervix (DiSaia &
3 Creasman, 1989; Fletcher & Hamberger, 1980; Powell, 2010). Definitive treatment most often consists of fractionated
4 external beam radiotherapy (EBRT) in combination with multi-fraction high-dose-rate (HDR) image-guided
5 intracavitary brachytherapy (IG-ICBT). Although the use of 3D imaging in gynaecological brachytherapy treatment
6 planning was first reported over 25 years ago (Ling, et al., 1987) it has only become routine clinical practice in the
7 past ten to fifteen years (Tanderup, et al., 2010; Pavamani, et al., 2011). With the advantages of image-based treatment
8 planning, it is possible to calculate the dose at every voxel of the image and delineate soft tissue structures. Therefore,
9 within the limits of uncertainty in structure delineation, dose delivered to organs at risk (OAR) such as the bladder,
10 rectum, uterus, vagina, and paracervical tissues can be determined with precision for each treatment fraction. These
11 capabilities have been recognized in the standard recommendations for image-based dose recording and a number of
12 dose volume histogram (DVH)-based parameters for both target and OAR volumes have been recommended for dose
13 reporting (Nag, et al., 2004; Nag, 2006; Haie-Meder, et al., 2005; Pötter, et al., 2006).

14 However, the ability to quantify the accumulated dose received by defined regions of tumour or normal structure
15 volumes over multiple radiotherapy fractions remains limited due to significant variations in the size and relative
16 positions of most, if not all, of these structures from one fraction to the next. These variations are caused by factors
17 such as variable bladder, bowel, and rectal filling, tumour regression, and displacement of structures by the
18 intracavitary brachytherapy apparatus. Thus, the GYN GEC-ESTRO task group (Pötter, et al., 2006) has advised that
19 consistent bladder filling volumes be used for valid and reliable data collection. However, varying the amount of
20 bladder filling in consecutive fractions has the potential to change the location of the hotspots on the bladder wall in
21 consecutive fractions, thereby limiting the magnitude of cumulative dose maxima over the course of treatment. Use
22 of large bladder filling volumes can also significantly reduce the cumulative dose to the other OAR, such as bowel,
23 with no significant difference in the dose distribution delivered to the target volume (Yamashita, et al., 2012; Patra, et
24 al., 2013; Harmon, et al., 2016; Whitley, et al., 2013).

25 Therefore, in order to reduce the overall dose maxima to the bladder and optimize sparing of OAR on at least some
26 fractions, our centre has adopted the practice of varying the amount of bladder filling in consecutive IG-ICBT fractions
27 for cervical cancer patients. In doing so we recognize that the bladder size variation is expected to cause larger
28 discrepancies between the actual cumulative dose and conventional plan-summed DVH parameters than a regimen in
29 which a consistent (e.g. empty) bladder filling is used (Pötter, et al., 2006; Andersen, et al., 2013; Teo, et al., 2015).
30 An additional limitation of current methods of dose accumulation is that DVH parameters are usually calculated for
31 the whole volume of the hollow OAR, including its fluid contents, whereas only the wall tissue is of radiobiological
32 interest. For these reasons, it is clear that more accurate methods and new dosimetric parameters are needed to replace
33 summed DVH parameters for estimating accumulated dose within the hollow organ walls in situations of repeated
34 fractions with changes in organ shape or size.

35 One of the known late effects of ICBT for locally advanced carcinoma of the cervix is urinary disorder. While
36 several studies have examined the relationship between dose and urinary toxicity in EBRT treatment or brachytherapy
37 for prostate cancer (Nilsson, et al., 2004; Rosewall, et al., 2010; Boersma, et al., 1998; Cheung, et al., 2007; Harsolia,
38 et al., 2007; Cozzarini, et al., 2012; Konishi, et al., 2009), there have been only a few dosimetric studies of urinary
39 toxicity for BT in cervical cancer patients (Georg, et al., 2011; Georg, et al., 2012; Wiebe, et al., 2010; Chen, et al.,
40 2009; Mazoner, et al., 2015, and a few others). Georg et al analyzed DVH-summed D_{2cm^3} , D_{1cm^3} , and $D_{0.1cm^3}$
41 parameters (in terms of equivalent dose in 2 Gy fractions) as predictors of late urinary toxicity in a cohort of 141
42 patients treated with EBRT and IG ICBT. They found a significant dose effect for all summed DVH parameters when
43 comparing groups with minor toxicity (Grade 0-1) to those with major toxicity (Grade 2-4). Mazoner et al found a
44 statistically significant association between urinary morbidity and DVH-summed D_{2cm^3} and $D_{0.1cm^3}$ in pulsed-dose
45 rate brachytherapy. However, studies examining the relationship between the true locally accumulated bladder dose
46 and bladder complications in cervical patients are still lacking.

1 The purpose of the study reported herein was to develop a method to more accurately accumulate the fractionated
2 dose in the bladder wall in HDR IG-ICBT for carcinoma of the cervix. It is hypothesized that the locally-accumulated
3 dose parameters are significantly different from the equivalent DVH-summed parameters, particularly when bladder
4 filling is varied between fractions. In addition, the locally-accumulated dose parameters were retrospectively studied
5 as predictors of the observed bladder toxicity. For dose accumulation, the correspondence between the bladder
6 structures in different fractions was estimated using a deformable point-set registration (PSR) method, called coherent
7 point drift (CPD). A software implementation of the CPD algorithm, proposed by Myronenko et al. (2010), is
8 available as a toolbox for MATLAB (The MathWorks Inc., Natick, MA, version R2013b), with adjustable registration
9 parameters. The performance of CPD was thoroughly investigated in a recent study (Zakariaee, et al., 2016) against
10 four other PSR methods and the deformable image registration (DIR) utility in the MIM Maestro software (MIM
11 Software Inc. Cleveland, OH, version 6.6.5), for registering surface contour points of a porcine bladder filled with
12 varying amounts of liquid. CPD showed the lowest average target registration error (TRE) of 6.4 mm amongst all
13 methods.

14 Similar attempts to accumulate radiotherapy fractionated dose in highly deformable organs such as bladder and
15 rectum have been reported in the literature (Yan, et al., 1999; Brock, et al., 2003; Andersen, et al., 2012; Andersen, et
16 al., 2013; Noe, et al., 2011; Xiong, et al., 2006; Georg, et al., 2011; Sabater, et al., 2014; Teo, et al., 2015; Jamema, et
17 al., 2015). Three of the most relevant studies were by Andersen et al. (2013), Jamema et al. (2015), and Teo et al.
18 (2015). Andersen et al. used a biomechanical DIR algorithm to locally accumulate the BT radiation dose on bladder
19 in 47 cervical cancer patients receiving fractionated EBRT and two sessions of IG BT. They compared the DIR-based
20 and DVH-based D_{2cm^3} and $D_{0.1cm^3}$ parameters and found the DVH-based parameters to be $(1.5 \pm 1.8)\%$ and $(5.2 \pm$
21 $4.2)\%$ larger than the DIR-based, respectively. Jamema et al. used an intensity-based and contour-based DIR for
22 deformable dose accumulation for bladder and rectum in two-fraction IGBT treatment of cervical cancer. They
23 compared the DIR-based D_{2cm^3} values to the DVH-summed D_{2cm^3} . Teo et al. performed a similar study on the data
24 from 20 patients treated with EBRT and 4-5 fractions of IG-ICBT, using MIM's DIR. They found a larger difference
25 of $(7.2 \pm 6.3)\%$ between DVH-based and DIR-based D_{2cm^3} . To the best of our knowledge, there have been no studies
26 that collectively i) look at the accumulated dose in the 'bladder wall' rather than the 'bladder surface', ii) apply
27 deformable 'point-set' registration using 'contour' data rather than 'image' data, and iii) study the relationship between
28 the bladder 'toxicity' and its geometrically-localized accumulated dose. The present study aims to meet all the above
29 criteria.

30 **Materials and Methods**

31 *Patient Materials and Contour Processing*

32 The treatment planning data for 60 cervical cancer patients receiving fractionated EBRT plus five HDR CT-based IG-
33 ICBT fractions (using a tandem/ring applicator for most cases and tandem/ovoid for some), were studied
34 retrospectively. This study was approved by the University of British Columbia Research Ethics Boards, certificate
35 number H1202320. All dose calculations were performed using the Eclipse™ and BrachyVision™ treatment planning
36 software (Varian Medical Systems Inc., Palo Alto, CA, version 13.0). The prescribed minimum peripheral dose to the
37 clinical target volume (CTV) was 600 cGy per HDR fraction for the vast majority of cases, with a few cases receiving
38 300-550 cGy in one, two or three out of five fractions, usually due to patient-specific factors such as extent and location
39 of the CTV. However, it must be noted that the toxicity assessment in this study was carried out relative to the
40 registered dose data and not the prescribed dose, and thus the actual prescription does not affect this analysis.

41 All patients received 45 Gy in 25 EBRT fractions, prescribed to the ICRU reference point (ICRU Report 62, 1999).
42 The EBRT planning was performed on a single planning CT image set and the patients were not imaged prior to each
43 fraction. However, the patients were instructed to fill their bladder prior to treatment (by drinking 0.5 liter of fluid an
44 hour before treatment and no voiding) and, therefore, roughly the same bladder filling regimen can be assumed for all
45 EBRT treatment fractions. The mean EBRT dose to bladder, based on the initial planning data, was on average 43.6

1 Gy. Due to the small inter-patient variations in the bladder EBRT dose (~5%), the EBRT component was not included in the dosimetric analysis in this study.

3 A Foley-Catheter was used to control bladder filling during HDR planning and delivery. Immediately prior to acquisition of the planning CT, and then again immediately prior to treatment delivery, the bladder was emptied using a syringe connected to the catheter, then another syringe containing the desired volume of fluid was used to fill the bladder. The catheter tube was then secured with a plastic clamp. A water-contrast mixture [3 cm³ of ISOVUE contrast agent (Bracco Diagnostic, Inc. Monroe Township, NJ) per 60 cm³ of sterile water) was used for the planning CT, and water alone was used for treatment. The aim was to vary the bladder filling volume from fraction to fraction by alternating the amount of fluid injected between 60 cm³ and 300 cm³. In practice, this was not always achievable due to factors such as residual urine in bladder and intolerance of some patients to larger volumes. Also, in some patients, the bladder was purposely kept full to avoid higher doses to small bowel. The fluid volume was recorded for each fraction.

13 For the purposes of this study, the bladder inner and outer surfaces were retrospectively re-contoured by a single observer (RZ) on the planning CT images of all brachytherapy fractions using the MIM Maestro software. This was done to ensure the highest possible accuracy and consistency of contouring (as the contours used for treatment planning had been generated with tight time constraints by various observers), and to obtain both inner and outer bladder wall contours. As a quality assurance indicator, the volume of the bladder-wall tissue was monitored during the contouring process, with the assumption that it should remain reasonably constant for each patient regardless of degree of distension - i.e. distension causes the wall to become thinner, but total wall volume stays constant.

20 The points of attachment of the urethra, as well the two ureters for the cases with CT images of adequate quality, were identified at each scan, and used as anatomical landmarks for accuracy assessment of the deformable registration. These landmarks were well suited for this purpose since they are located in the posterior part of the bladder where the highest dose regions tend to occur. As an additional quality assurance check, a random selection of the bladder-wall contours and landmark points, equivalent to 10% of the cases, were reviewed and approved by a radiologist. For each patient, the bladder inner and outer surfaces and the dose matrix associated with each HDR fraction was imported into MATLAB. The bladder-wall structure was then built by linearly interpolating between neighbouring inner- and outer-surface points so as to form four additional shells in between.

28 CPD Deformable Point-set Registration

29 The detailed description, attributes and optimal parameter settings of the CPD toolbox for registering bladder contour point-sets have been previously published (Zakariaee, et al., 2016). The same procedure and optimal settings of the registration parameters were used in this study, with one main difference. In this study, the *reference* point-set was the *moving* (i.e. deforming) structure, in contrast to the previous procedure, where the *reference* point-set was the *target* (i.e. fixed) structure. This was because, in order to locally accumulate (i.e. register) the fraction doses on the contour points of a single (*reference*) structure, a correspondence must be found for all the points in that point-set. Therefore, CPD was used to register the *reference* point-set to the other four *target* point-sets, finding a match for every *reference* point to another point in each of the *target* point-sets.

37 The *TRE* value for each anatomical landmark was calculated, for every registration, as the distance between the matched point in the *target* point-set and the known position of the corresponding landmark in *reference*. In order to remove the effect of distension of the chosen reference structure on the scaling of the *TRE* values, a normalized registration error (*NRE*) was defined using the equation,

$$41 \quad NRE = TRE \times \frac{ES \text{ radius of smallest volume}}{ES \text{ radius of reference volume}}, \quad (1)$$

42 where *ES* is the equivalent sphere of the corresponding volume. The *NRE* values for all four registrations and across three landmarks were averaged to derive a *NRE*_{avg}. For each subject, the bladder point-set derived from each of the five fractions was tested as the *moving* structure and a *NRE*_{avg} was calculated for each scenario. The fraction yielding

1 the smallest NRE_{avg} value was chosen as the *reference* fraction for the dose registration, in order to minimize the
2 registration uncertainty.

3 *Dose Accumulation*

4 After establishing the point correspondence, the point-dose values were calculated for each fraction by linear
5 interpolation of the voxel-dose values, assuming locally-linear decay of dose in regions away from the steep dose
6 gradients closer to the brachytherapy sources. This was confirmed to be a reasonable approximation by comparison
7 with doses calculated by BrachyVision for a series of test points. The registered point-dose values for all the points in
8 the *reference* point-set were calculated using

$$9 \quad rD_p = \sum_{i=1}^5 d_{p,i}, \quad (2)$$

10 where rD_p is the registered dose at point p and $d_{p,i}$ is the dose at point p in fraction i . The registered doses were also
11 calculated as biologically weighted, 2 Gy fraction equivalents (EQD2), derived using the linear quadratic model (α/β
12 = 3 Gy) (Fowler, 1989; Dale & Jones, 1998),

$$13 \quad rEQD2_p = BED_p / (1 + \frac{2}{\alpha/\beta}), \quad (3)$$

14 where

$$15 \quad BED_p = \sum_{i=1}^5 [d_{p,i} (1 + \frac{d_{p,i}}{\alpha/\beta})] \text{ (Lang, et al., 2007)}. \quad (4)$$

16 In order to create a ‘solid’ bladder-wall and accumulate the dose at each ‘voxel’ of bladder-wall, the *reference*
17 bladder-wall contour was rasterized into an image volume (binary mask of the bladder-wall) with the same size and
18 resolution as the planning CT images. The accumulated voxel-dose values were then approximated by linear
19 interpolation of the rD_p values of five nearest neighbouring points at the position of each bladder-wall mask voxel,
20 creating a cumulative dosage mask (Fig. 1). The same method was applied to find the EQD2 dosage mask. Note that,
21 as discussed above, the bladder tissue volume is consistent and equivalent across different fractions, so the choice of
22 reference fraction should not affect the absolute values of the computed dose-volume parameters.

23 *Registered Dosimetric and Volumetric Parameters*

24 Because the registered cumulative dose distributions often exhibited separated, non-contiguous high dose regions, the
25 search for critical high-dose volumes on the bladder wall that might explain the observed severe bladder toxicity in
26 some patients included dosimetric parameters calculated for contiguous high dose regions. In order to find contiguous
27 volumes of high dose (i.e. *hotspots*) on the bladder wall, a novel region growing algorithm was developed in-house,
28 using a Random Walker (RW) software¹ to enforce smoothness on the calculated regions around the high-dose voxels.
29 This algorithm was used to calculate the minimum registered dose to the contiguous high-dose $n\text{-cm}^3$ of the bladder
30 wall, rD_{ncm^3} , for 1 and 2 cm^3 volumes. In addition, conventional DVH-based (i.e. non-contiguous) rD_{ncm^3} were
31 calculated for volumes recommended by GYN GEC-ESTRO guidelines for OARs (0.1, 1, and 2 cm^3 ; optional 5 and
32 10 cm^3) (Pötter, et al., 2006), with the exclusion of the 0.1- cm^3 volume because its dimensions were comparable to
33 the registration uncertainties. However, it must be noted that the 5 and 10 cm^3 registered dose volumes were generally
34 contiguous.

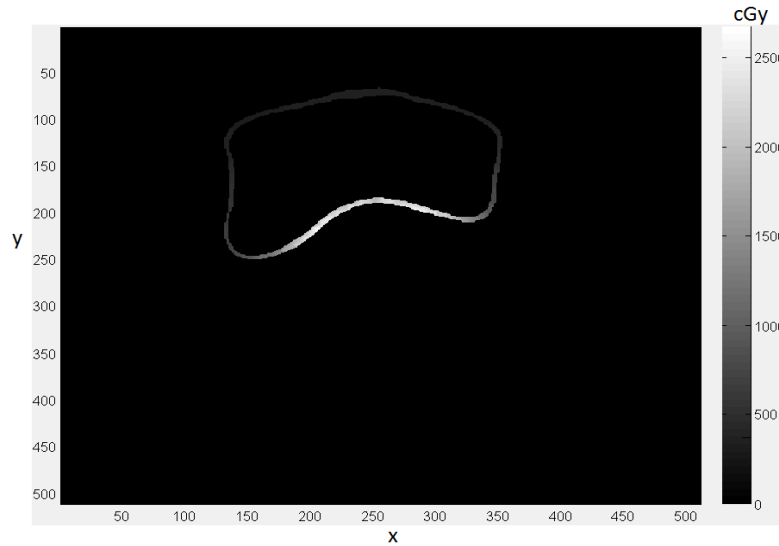
35 Also calculated were the non-contiguous volume of the bladder wall receiving a minimum registered dose of n
36 Gy, rV_{nGy} (evaluated for 3, 5, and 10 Gy), $rEQD2_{ncm^3}$ parameters for 1 and 2 cm^3 (contiguous), and 5 and 10 cm^3
37 (DVH-based) volumes in the EQD2 dosage mask, and the mean and integral dose to the bladder wall. Table 1 shows
38 a list of all the dosimetric and volumetric parameters calculated in this study, with their definitions. Conventional
39 plan-summed parameters, sD_{ncm^3} , were calculated using the DVH data from the treatment planning software for each
40 fraction and summing across all fractions. Because they were based solely on DVH data, sD_{ncm^3} were not spatially
41 defined.

¹ Fast Random Walker by Shawn Andrews et al. (2010), available at <http://fastrw.cs.sfu.ca/>.

1 *Urinary Toxicity Scoring and Statistical Analysis*

2 Post-treatment late effects in bladder were assessed based on the Late Effects in Normal Tissues–Subjective,
 3 Objective, Management and Analytic (LENT-SOMA) scale (Rubin, et al., 1995), collected from the patients over the
 4 course of their post-treatment follow-up. No baseline (pre-treatment) urinary complication data were collected for this
 5 cohort. The overall urinary toxicity scores were recorded as the average of the LENT-SOMA grades for endpoints
 6 including frequency, urgency, incontinence, hematuria, dysuria, nocturia, and change in stream. The toxicity scores
 7 ranged from 0.00 to 4.00. The subjects with overall toxicity scores >1.5 (i.e. Grade 2-4) were placed into the Case
 8 group and those with scores <1.5 (i.e. Grade 0-1) into the Control group. This choice of cut-off point for a clinically
 9 significant late toxicity was based on previous studies showing significant dose effect for complication grades ≥ 2
 10 (Georg, et al., 2011; Georg, et al., 2012).

11 The descriptive statistics for the dosimetric and volumetric parameters were recorded for the Case and Control
 12 groups separately. A two sample t-test analysis was performed at a 5% level of significance for all dose parameters,
 13 with the null hypothesis of equal means for the Case and Control groups. In addition, a binomial logistic regression
 14 analysis was performed using SPSS Statistics software (IBM Corp. Armonk, NY, version 14.0), to investigate the
 15 effect of each registered dose parameter on urinary toxicity. This was achieved by assigning a 0/1 dose category to
 16 each patient (Control=0, Case=1).



17
 18 **Figure 1.** A cross section of a bladder-wall cumulative dosage mask, showing the distribution of voxel doses as
 19 different shadings in the mask, with the brighter regions having a larger registered dose than the darker ones.

20 **Table 1.** Bladder wall dosimetric and volumetric parameters included in this study.

Parameter	Definition
rD_{ncm^3}	Minimum registered dose to the contiguous or non-contiguous high dose $n\text{-cm}^3$ volume ($n=1-10$)
$rEQD2_{ncm^3}$	Minimum registered EQD2 dose to contiguous or non-contiguous high dose $n\text{-cm}^3$ volume ($n=1-10$)
rV_{nGy}	Non-contiguous volume receiving a minimum registered dose of n Gy ($n=3-10$)
M_{dose}	Mean registered dose
I_{dose}	Integral registered dose ($\sum_i d_i m_i$, where m_i is the mass of each voxel and d_i is its registered dose)
sD_{ncm^3}	Summed D_{ncm^3} from DVH data ($\sum_{i=1}^5 rD_{ncm^3,i}$, where i =fraction number)
$sEQD2_{ncm^3}$	Summed $EQD2_{ncm^3}$ from DVH data ($\sum_{i=1}^5 rEQD2_{ncm^3,i}$, where i =fraction number)

1 Volume Variation Effect

2 The intra-patient variation of the bladder volume (i.e. wall tissue plus lumen) over the five fractions, *VolVar*, was
3 defined as (maximum-minimum)/minimum of the filling volumes. Also, in order to assess the anatomical movement
4 of the hotspots on the bladder, the location of the hottest point on each fraction was mapped to the reference bladder
5 using the registration outputs. Then, the mean and maximum of all the distances between different pairs of hottest
6 points for the five fractions were calculated. To evaluate the effectiveness of varying the bladder filling in moving the
7 hotspot regions on the bladder and reducing urinary toxicity, a linear regression analysis was performed between (i)
8 the mean and maximum hotspot distances and *VolVar*, and (ii) urinary toxicity score (on a 0.00-4.00 scale) and *VolVar*.
9 For both analyses, the p-values for a non-zero slope of the linear regression were calculated.

10 Results

11 The observed bladder LENT-SOMA toxicity scores across all subjects ranged from 0.00 to 3.57 (i.e. Grade 0-4). The
12 toxicity scores in the Case group ranged from 1.57 to 3.43, with an average of 2.02 ± 0.61 and those in Control ranged
13 from 0.00 to 1.43, with an average of 0.81 ± 0.43 . The difference between the toxicity scores of Case and Control
14 groups was significant ($p < 0.000001$). The mean EBRT dose values (*mEBRT*) received by the bladder were determined
15 based on the initial planning data. The coefficient of variation of the *mEBRT* values was only 5% across all cases. The
16 mean *mEBRT* values for the Control and Case groups were $43.3 \pm 9\%$ Gy and $44.2 \pm 3\%$ Gy, respectively.

17 All registrations were visually inspected and found to be reasonable (i.e. no extreme outliers could be identified).
18 For most of the cases, the overall match was quite satisfactory with small apparent discrepancies (see Fig. 2 for an
19 example). Quantitatively, the *NRE_{avg}* values (for the optimal *reference* fraction, as described previously) ranged from
20 2.4 mm to 9.2 mm across all subjects, with a mean of 4.8 ± 1.5 mm. The per-fraction and registered dose distributions
21 on the bladder-wall contour point clouds, for the same case as in Fig. 2, are shown in Fig. 3. It must be noted that since
22 the maximum bladder dose varied among different fractions (for this case from ~ 400 cGy in Fraction 2 to ~ 770 cGy
23 in Fraction 5), using the same isodose scale for all fractions causes the hotspots to appear as cyan/green shades rather
24 than red/maroon for most of the fractions. It can be seen that the locations of the hotspots vary significantly for most
25 of the fractions and, therefore, the location of the summed hotspot is quite different from per-fraction hotspot locations.
26 This confirms the conjecture that simply adding the unregistered dosimetric parameters will not provide an accurate
27 estimate for the magnitude or spatial distribution of the cumulative dose over all fractions.

28 The per-patient, inter-fraction variation of bladder-wall tissue volume was low with an average of $(5.4 \pm 1.6)\%$ and
29 a maximum of 8%. The average bladder-wall thickness over all fractions of all subjects was found to be 3 ± 1 mm. The
30 range of bladder filling volumes across all fractions and all patients was 71-562 cm³. The maximum intra-patient
31 volume variation (maximum volume-minimum volume) ranged between 4.5-427 cm³, with a mean of 152 ± 112 cm³.
32 The degree of volume variation as measured by *VolVar* ranged between 3.7% and 353.3% across all cases, with an
33 average of $(104 \pm 86)\%$. The slope of the regression line for urinary toxicity score versus *VolVar* was -0.23 ($p=0.03$).
34 The ranges of the mean and maximum hotspot separation distances across all cases were 3-38 mm and 5-67 mm,
35 respectively. It must be noted that these separation distances are Euclidean distances and not a geodesic shortest path
36 on the surface on the bladder. Therefore, these distances may be an underestimation of the actual distances between
37 the hotspots along the bladder surface, particularly for cases where the hotspots occur in different lateral horns of the
38 bladder. The slopes of the regression lines for the mean and maximum hotspot separations as a function of *VolVar*
39 were, respectively, 3.8 mm ($p=0.03$) and 7.1 mm ($p=0.002$).

40 The DVH-based (non-contiguous) rD_{ncm^3} values for 1 and 2 cm³ volumes were $(5 \pm 3)\%$ and $(3 \pm 2)\%$ lower than
41 the corresponding DVH-based sD_{ncm^3} values, respectively, while the contiguous rD_{ncm^3} values for 1 and 2 cm³ were,
42 on average, $(16 \pm 5)\%$ and $(18 \pm 5)\%$, smaller than the equivalent sD_{ncm^3} parameters. The contiguous $rEQD2_{ncm^3}$
43 values were, on average, $(26 \pm 10)\%$ and $(27 \pm 11)\%$, smaller than the equivalent DVH-based $sEQD2_{ncm^3}$ parameters
44 for 1 and 2 cm³ volumes, respectively.

45

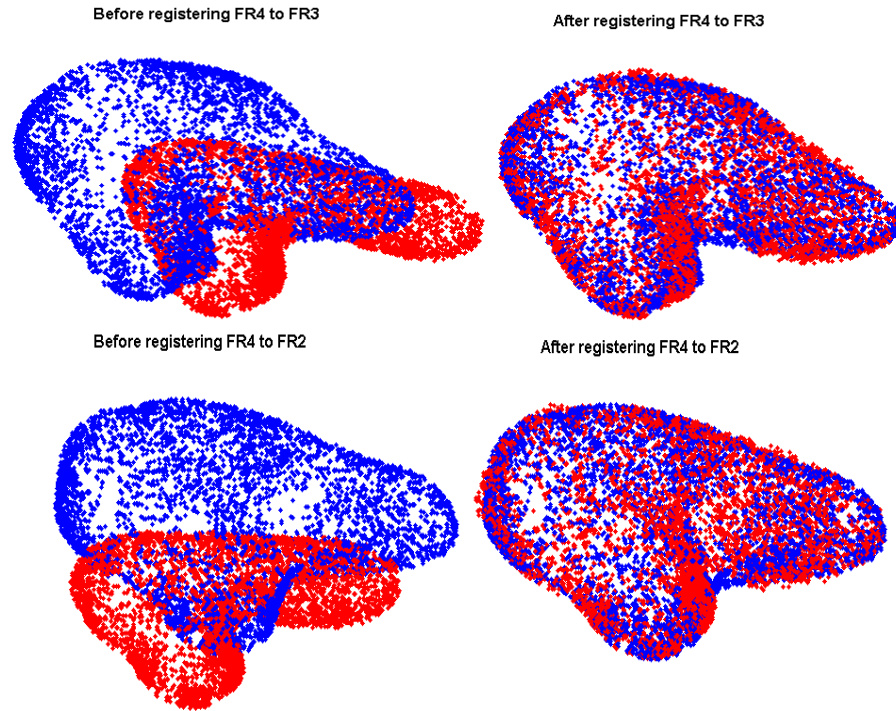


Figure 2. Example of the registration outcomes for registering the *reference* bladder-wall contour point-set (FR4) to two larger fractions (FR2 and 3): ‘Before’ and ‘After’ scenarios.

Table 2 shows the results for a selection of the registered dosimetric and volumetric parameters for the Case and Control groups. It can be seen that for all parameters, except one, the mean value for the Case group is higher than the Control group, as expected. V_{3Gy} demonstrated a significant difference between Case and Control means based on two sample t-test at a 5% level of significance ($p=0.016$). rV_{5Gy} and I_{dose} showed a significant difference at the 10% level. The t-test analysis was also performed for the sD_{ncm^3} and $sEQD2_{ncm^3}$ parameters and the most significant result was observed for $sEQD2_{10cm^3}$ with a p-value of 0.097.

Table 3 shows the results of the univariate logistic regression analysis for selected registered dosimetric and volumetric parameters, including the p-value, odds ratio (OR), and the 95% confidence interval (CI) lower and upper limits. Based on these results, only V_{3Gy} ($p=0.015$) might be a predictor of Grade 2-4 urinary toxicity; however, the increased odds of having a urinary toxicity grade of larger than 2 with higher values of V_{3Gy} is borderline (OR=1.075, 95% CI=1.014-1.140).

Discussion

In this study, deformable PSR utility of the CPD toolbox was applied to bladder-wall contour point sets of five treatment fractions for 60 cervical HDR brachytherapy patients. The quality of the registration outcomes was confirmed both visually and through the landmark registration errors using three anatomical points on the bladder surface. The PSR results were used to accumulate the dose on the bladder wall of a reference fraction and registered dosimetric and volumetric parameters were computed. The unregistered, DVH-summed dosimetric parameters commonly used in clinical practice were also calculated and compared to the registered-dose parameters. The dosimetric and volumetric parameters were then evaluated as predictors of urinary toxicity grades.

1 **Table 2.** The Case (CS) and Control (CN) statistics for selected dosimetric and volumetric parameters, based on registered dose, and the bladder volume variation in
 2 percentage. The p-values less than 0.1 are highlighted in bold text.

	$rD_{1cm^3}^*$ (Gy)		$rD_{2cm^3}^*$ (Gy)		rD_{5cm^3} (Gy)		rD_{10cm^3} (Gy)		$rEQD2_{1cm^3}^*$ (Gy)		$rEQD2_{2cm^3}^*$ (Gy)		$rEQD2_{5cm^3}$ (Gy)		$rEQD2_{10cm^3}$ (Gy)		rV_{3Gy} (cm ³)		rV_{5Gy} (cm ³)		rV_{10Gy} (cm ³)		I_{dose} (Gy)		M_{dose} (Gy)		$VolVar$ (%)	
	CS	CN	CS	CN	CS	CN	CS	CN	CS	CN	CS	CN	CS	CN	CS	CN	CS	CN	CS	CN	CS	CN	CS	CN	CS	CN	CS	CN
Mean	21.7	21.9	19.8	19.2	19.0	18.5	14.1	13.0	34.7	33.1	29.5	27.0	27.9	26.0	17.7	15.3	50.9	43.0	35.5	30.8	16.0	14.1	484	419	9.0	9.0	21.3	27.1
Median	21.9	21.5	20.3	19.4	19.3	18.9	13.5	12.6	34.1	33.6	28.3	25.9	27.4	27.3	16.3	15.4	50.2	41.0	32.6	31.6	15.1	14.1	431	419	9.1	8.7	20.6	27.3
Stdev	6.1	4.1	5.7	3.9	5.8	4.2	4.6	3.8	15.0	9.6	12.5	8.6	12.8	9.6	8.3	7.1	13.1	8.9	13.0	9.5	7.4	5.3	173	128	2.4	2.1	3.6	2.3
Min	9.9	12.8	8.8	10.9	8.5	10.9	6.6	7.0	9.7	13.5	8.4	11.1	8.2	8.6	5.8	4.4	27.2	23.9	17.2	15.1	2.4	5.7	233	195	4.9	5.2	3.4	1.5
Max	32.5	30.1	29.1	28.4	29.7	29.5	21.4	24.5	68.7	51.6	55.0	51.0	55.4	53.8	31.2	40.0	75.9	62.5	61.7	55.6	30.1	29.7	778	829	12.7	13.4	44.6	51.8
p-value	0.461		0.345		0.375		0.188		0.343		0.223		0.294		0.156		0.016		0.092		0.182		0.087		0.489		0.078	

3 * parameter is calculated for a contiguous dose volume

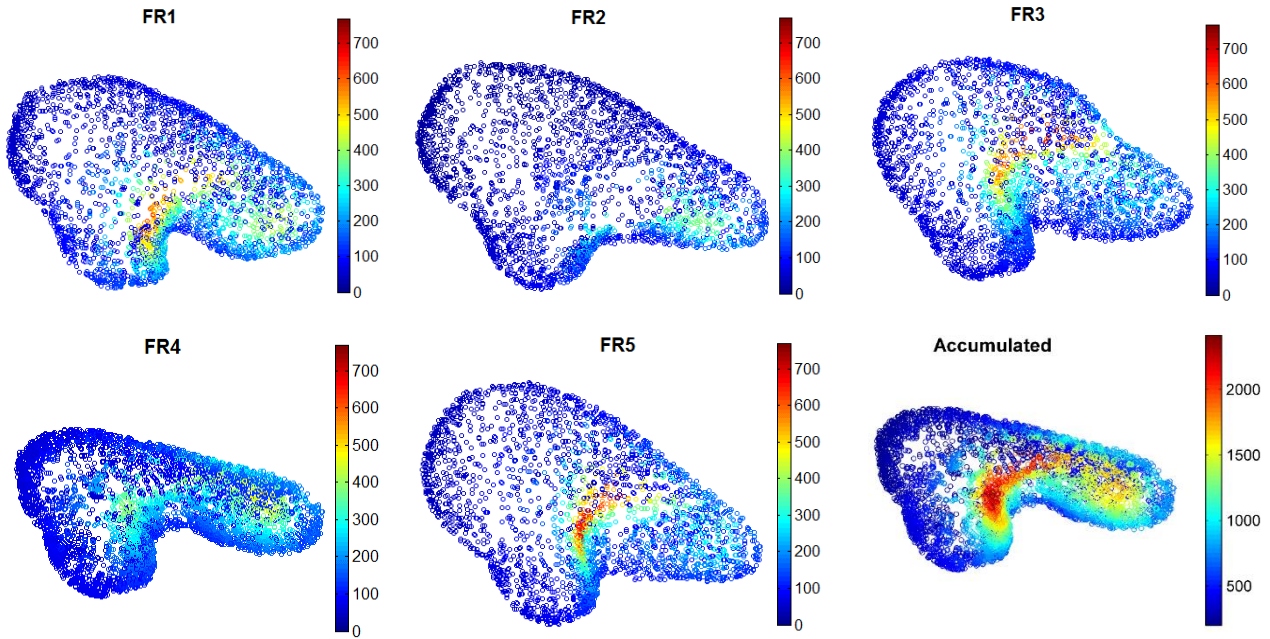
4 **Table 3.** Logistic regression outcomes for selected dosimetric and volumetric parameters, showing the odds ratio (OR), lower and upper limits of 95% confidence
 5 interval (CI), and the p-values. The p-values less than 0.05 are highlighted in bold text.

	$rD_{1cm^3}^*$	$rD_{2cm^3}^*$	rD_{5cm^3}	rD_{10cm^3}	$rEQD2_{1cm^3}^*$	$rEQD2_{2cm^3}^*$	$rEQD2_{5cm^3}$	$rEQD2_{10cm^3}$	rV_{3Gy}	rV_{5Gy}	rV_{10Gy}	I_{dose}	M_{dose}
OR	1.004	1.071	1.111	1.197	1.015	1.030	1.061	1.094	1.075	1.042	1.053	1.003	0.996
95% CI	0.880-1.145	0.921-1.246	0.940-1.313	0.966-1.483	0.962-1.070	0.969-1.094	0.972-1.159	0.961-1.246	1.014-1.140	0.988-1.099	0.958-1.157	0.999-1.007	0.763-1.299
p-value	0.954	0.374	0.218	0.100	0.586	0.343	0.184	0.174	0.015	0.127	0.286	0.120	0.976

6 * parameter is calculated for a contiguous dose volume

7

1



2

3 **Figure 3.** The per-fraction and accumulated point-dose distributions, on the same geometrical and isodose scale, for
4 the representative case in Fig. 2. The prescription dose for this case was 600 cGy for fractions 1,3,4 and 5, and 500
5 cGy for fraction 2. The accumulated dose over all fractions is displayed on the reference fraction (FR4).
6

7 The registration uncertainty achieved in this study (4.8 ± 1.5 mm) is amongst the best reported values for bladder
8 deformable registration (Chen, et al., 2016; Wognum, et al., 2014; Zakariaee, et al., 2016). It has been shown
9 previously (Zakariaee, et al., 2016) that CPD has superior registration accuracy compared to five other PSR
10 techniques, including a widely used method called thin-plate spline robust point matching (TPS-RPM). In a recent
11 study, Chen et al. (2016) has developed an improved TPS-RPM method with local topology preservation, for the
12 purpose of bladder dose accumulation in cervical cancer HDR brachytherapy. They tested their method on three
13 different sets of data: synthetic data, porcine bladder phantom (using fiducials), and patient data (using bladder neck
14 landmark). While they reported residual distance errors (RDE) of 3.7 ± 2 mm on average, for both porcine bladder and
15 patient data, the amount of variation in bladder size in that study (80 - 300 cm³ total volume) was much less than the
16 variations tested in the current study (i.e. 71 - 562 cm³). Given that it has been shown that the registration error becomes
17 larger with the variation in structure dimensions (Chen, et al., 2016; Wognum, et al., 2014; Zakariaee, et al., 2016), a
18 slightly larger registration error is expected in our work.

19 According to the phantom-based PSR validation study (Zakariaee, et al., 2016), the registration uncertainty for
20 CPD is more tangential than transverse. Therefore, the average *NRE* error reported in our current clinical study can be
21 compared against the planar dimensions of the measured hotspot volumes. Considering the average bladder-wall
22 thickness of 3 mm, the square-shaped planar dimension of the smallest high-dose volume considered (i.e. 1 cm³) is
23 about 18.3 mm. This size is 3.8 times the average registration error of 4.8 mm, suggesting that although this registration
24 uncertainty in the achieved hotspot might cause some smearing and blurring of the edges, the hotspot region in each
25 fraction would still be mostly aligned. Moreover, since the dose fall-off is more gradual in the bladder than it is in
26 regions closer to the sources, there are no drastic variations in dose values across a 5-mm distance on the bladder
27 surface. Furthermore, as the hotspot volume increases to 2, 5 and 10 cm³, the planar dimensions expand to 26, 41, and
28 58 mm, diminishing the impact of the registration uncertainty even further. Revisiting Fig. 3, it is clear that

1 accumulation of dose, after performing registration, is far more accurate than assuming total overlap of the hotspots
2 and simply summing their DVH dose parameters, despite minor uncertainties in registration.

3 Based on the results of this study, the unregistered, summed D_{2cm^3} overestimates the cumulative contiguous
4 hotspot dose by $(18\pm 5)\%$. This difference was much lower for the registered non-contiguous dose, i.e. $(3\pm 2)\%$, which
5 is comparable to the results previously reported by Andersen et al. (2013), Jamema et al. (2015), and Teo et al. (2015),
6 i.e. $(1.5\pm 1.8)\%$, $(5.2\pm 5.1)\%$, and $(7.2\pm 6.5)\%$, respectively. As previously discussed in Andersen et al. (2013), some
7 overestimation of dosimetric parameters from DVH summation is expected because adding, for example, the per-
8 fraction D_{2cm^3} values assumes that the same 2 cm^3 on the bladder wall is receiving the highest dose over all treatment
9 fractions. This assumption is referred to as the “worst case assumption” in the GYN GEC-ESTRO recommendations
10 (Haie-Meder, et al., 2005; Pötter, et al., 2006). As observed in our study, the differences are even larger when doses
11 to contiguous hot spots are considered. The differences between the contiguous registered dose and the DVH-summed
12 parameters appear to be largely attributable to the inherent difference in these two parameters when hot spots are
13 distributed over the volume of interest, since the contiguous volume analysis captures some aspects of the spatial
14 distribution while conventional DVH-based analysis does not. This may also be of relevance in the dosimetric analysis
15 of single treatment fractions, since it is not uncommon for the bladder to have two separate hotspots due to the location
16 of the HDR applicator (and its corresponding dose distribution) with respect to the so-called ‘lateral horns’ (Pötter, et
17 al., 2006) of the bladder.

18 Using DVH-summed parameters for defining OAR dose thresholds may provide safe margins for OAR treatment
19 planning purposes and reduce the rate of observed urinary toxicity to a great extent (Georg, et al., 2011; Georg, et al.,
20 2012), but it failed to explain the observed toxicity in the cervical cancer patients treated with HDR brachytherapy at
21 our center. Being able to correctly accumulate the dose across treatment fractions may provide grounds for defining
22 new bladder dose thresholds that would better prevent the late urinary complications and/or allow better tailoring of
23 dose to the target volume. In this quest, an analysis was performed for 13 different dose parameters by separating the
24 subjects into Case and Control groups based on their overall bladder toxicity grades. While only one of the parameters
25 evaluated (rV_{3Gy}) yielded a significant rejection of the null hypothesis ($p=0.02$), it was found that 11 out of 13
26 parameters evaluated had higher means for the Cases compared to the Controls. The p-value for finding 11 out of 13
27 mean parameter values higher in the Cases than in the Controls is 0.002, which is quite significant. However,
28 considering that there are correlations between the parameters, they are not all independent.

29 The correlations between the test parameters and toxicity score were further studied using univariate binomial
30 logistic regression analysis. The outcomes of this analysis also suggested that only rV_{3Gy} might be a predictor for Grade
31 2+ urinary toxicity; however, the effect size in terms of odds ratio was not very large ($OR=1.075$). If the effect is real,
32 a possible underlying mechanism might be that the urinary endpoints that more effectively influence the average
33 toxicity score (i.e. frequency and urgency for our data set) are more strongly associated with larger volumes of the
34 bladder receiving accumulated doses beyond a certain threshold. Further investigation of this effect would benefit
35 from inclusion of baseline urinary complication data in the analysis in order to account for the effect of higher baseline
36 values that might exist for some patients.

37 In this study, the effectiveness of the practice of varying the bladder filling volume across different HDR BT
38 treatment fractions for the purpose of moving the location of the hotspots and reducing urinary toxicity was also
39 evaluated. It was observed that varying the bladder filling volume correlated significantly ($p=0.03$) with both hotspot
40 separation and urinary toxicity. This result suggests that varying the bladder filling regimen has the potential to reduce
41 the urinary toxicity by moving the location of the maximally irradiated regions on the bladder across different
42 brachytherapy treatment sessions.

43 The statistical power based on the Case and Control sample sizes for $\alpha=0.05$ is 0.95 for rV_{3Gy} , which is a strong
44 statistical power considering the accepted standard minimum of 0.80 for avoiding a type II error (i.e. false negative)
45 in rejecting a null hypothesis. However, given the total number of parameters tested, we recognize the chance of
46 *multiple comparisons problem* in our findings (Miller, 1981), causing a type I error (i.e. false positive). Therefore, we

1 applied Holm's *step-down approach* (Holm, 1979) for controlling the familywise error rate (FWER) (Tamhane, 1996)
2 and determined that no true rejected null hypotheses can be established from the results of this study. However, this
3 FWER calculation would represent the worst case scenario of considering all 13 parameters to be independent, which
4 is not the case as stated above. Nevertheless, we regard our findings at this stage to be hypothesis-generating only,
5 recognizing that analysis of a larger data set would be required in order to reach more definitive conclusions.

6 Although there was no difference observed in the bladder mean EBRT dose from the planning data between the
7 Case and Control groups, the EBRT dose can play an important role in the observed urinary late effects. Since there
8 was only a single planning image available for each patient and the patients were not imaged prior to each EBRT
9 fraction, the intra-fraction variations could not be accounted for. Therefore, it was not possible to register the EBRT
10 dose across treatment fractions. However, considering that a reasonably consistent bladder filling regimen can be
11 assumed for EBRT treatment fractions, the inter-fraction variations are believed to be small compared to the variations
12 seen for the brachytherapy treatments. That being said, no quality assurance or auditing of the bladder filling during
13 EBRT was performed. A more rigorous study of the dose effect relationship of the urinary late effects would require
14 data with repeated EBRT imaging in order to find the total accumulated dose distributions on the bladder from both
15 EBRT and brachytherapy. Moreover, as mentioned above, baseline urinary complication data is required for a more
16 accurate evaluation of post-treatment toxicity. Such information could potentially lead to a more definitive association
17 between urinary toxicity and registered dose parameters.

18 **Conclusion**

19 The results of this study show that DVH-summed parameters calculated from unregistered data sets overestimate the
20 bladder dose in intracavitary cervical HDR brachytherapy, particularly when contiguous high dose volumes are
21 considered and when large variations in bladder filling volume are present. Volumetric registered-dose parameters
22 with lower dose thresholds may have the potential to explain some of the severe urinary toxicity observed in certain
23 patients. While more research is required in order to fully characterize the dose effect relationship of late urinary
24 complications in cervical cancer patients treated with EBRT and multi-fraction HDR BT, deformable point-set
25 registration appears to be a viable tool for accurate dose accumulation in fractionated image-guided brachytherapy.

26 **Acknowledgements**

27 The authors would like to thank Dr. Monty Martin, BC Cancer Agency Department of Radiology, for teaching and
28 reviewing the landmark identification and the bladder contours. The authors would also like to thank Alborz Amir-
29 Khalili from the Electrical Engineering Department at the University of British Columbia for providing the algorithm
30 for measuring the most irradiated contiguous volumes using the Fast Random Walker software. We would also like
31 to thank Dr. Peter Lim, BC Cancer Agency Department of Radiation Oncology, for his valuable feedback on the
32 toxicity analysis.

33 **References**

- 34 Andersen, E., Muren, L. & Sørensen, T., 2012. Bladder dose accumulation based on a biomechanical deformable
35 image registration algorithm in volumetric modulated arc therapy for prostate cancer. *Phys. Med. Biol.*, 57(21), p.
36 7089.
- 37 Andersen, E., Noe, K. & Sørensen, T., 2013. Simple DVH parameter addition as compared to deformable
38 registration for bladder dose accumulation in cervix cancer brachytherapy. *Radiother. Oncol.*, 107(1), pp. 52-57.
- 39 Andrews, S., Hamarneh, G. & Saad, A., 2010. Fast Random Walker with Priors using Precomputation for
40 Interactive Medical Image Segmentation. *Lecture Notes in Computer Science, Medical Image Computing and*
41 *Computer-Assisted Intervention (MICCAI)*, pp. 9-16.

- 1 Boersma, L., Brink, M. V. d. & Bruce, A., 1998. Estimation of the incidence of late bladder and rectum
2 complications after high-dose (70-78 Gy) conformal radiotherapy for prostate cancer, using dose-volume
3 histograms. *Int. J. Radiat. Oncol. Biol.*, 41(1), pp. 83-92..
- 4 Brock, K., McShan, D. & Haken, R. T., 2003. Inclusion of organ deformation in dose calculations. *Med. Phys.*,
5 30(3), pp. 290-295.
- 6 Chen, H., Zhong, Z., Liao, Y. & Pompoš, A., 2016. A non-rigid point matching method with local topology
7 preservation for accurate bladder dose summation in high dose rate cervical brachytherapy. *Phys. Med. Biol.* , 61(3),
8 p. 1217.
- 9 Chen, S.-W. et al., 2009. Geometrical Sparing Factors for the Rectum and Bladder in the Prediction of Grade 2 and
10 Higher Complications After High-Dose-Rate Brachytherapy for Cervical Cancer. *Int. J. Radiat. Oncol. Biol.*, 75(5),
11 p. 1335–1343.
- 12 Cheung, M., Tucker, S. & Dong, L., 2007. Investigation of bladder dose and volume factors influencing late urinary
13 toxicity after external beam radiotherapy for prostate cancer. *Int. J. Radiat. Oncol. Biol.*, 67(4), pp. 1059-1065.
- 14 Cozzarini, C., Fiorino, C., Pozzo, L. D. & Alongi, F., 2012. Clinical factors predicting late severe urinary toxicity
15 after postoperative radiotherapy for prostate carcinoma: a single-institute analysis of 742 patients. *Int. J. Radiat.*
16 *Oncol. Biol.*, 82(1), pp. 191-199.
- 17 Dale, R. & Jones, B., 1998. The clinical radiobiology of brachytherapy. *Br. J. Radiol.*, 71(845), pp. 465-483.
- 18 DiSaia, P. & Creasman, W., 1989. *Clinical gynecological oncology*. 3rd ed ed. New York: C.V. Mosby.
- 19 Fletcher, G. & Hamberger, A., 1980. Squamous cell carcinoma of the uterine cervix: Treatment technique according
20 to size of the cervical lesion and extension. In: F. GH, ed. *Textbook of radiotherapy*. 3rd ed ed. Philadelphia: Lea &
21 Febiger, p. 732–772.
- 22 Fowler, J., 1989. A Review: The linear quadratic formula and progress in fractionated radiotherapy. *Br. J. Radiol.*,
23 62(740), pp. 679-694.
- 24 Georg, P., Lang, S., Dimopoulos, J. & Dörr, W., 2011. Dose–Volume Histogram Parameters and Late Side Effects
25 in Magnetic Resonance Image–Guided Adaptive Cervical Cancer Brachytherapy. *Int. J. Radiat. Oncol. Biol.*, 79(2),
26 pp. 356-362.
- 27 Georg, P., Pötter, R., Georg, D. & Lang, S., 2012. Dose Effect Relationship for Late Side Effects of the Rectum and
28 Urinary Bladder in Magnetic Resonance Image-Guided Adaptive Cervix Cancer Brachytherapy. *J. Rad. Onc. Biol.*
29 *Phys.*, 82(2), p. 653–57.
- 30 Haie-Meder, C., Pötter, R. & Limbergen, E. V., 2005. Recommendations from Gynaecological (GYN) GEC-ESTRO
31 Working Group (I): concepts and terms in 3D image based 3D treatment planning in cervix cancer brachytherapy
32 with emphasis on MRI assessment of GTV and CTV. *Radiother. Oncol.*, 74(3), pp. 235-245.
- 33 Harmon, G., Chinsky, B., Surucu, M. & Harkenrider, M., 2016. Bladder distension improves the dosimetry of
34 organs at risk during intracavitary cervical high-dose-rate brachytherapy. *Brachytherapy*, 15(1), pp. 30-34.
- 35 Harsolia, A., Vargas, C., Yan, D. & Brabbins, D., 2007. Predictors for chronic urinary toxicity after the treatment of
36 prostate cancer with adaptive three-dimensional conformal radiotherapy: Dose-volume analysis of a phase II dose-
37 escalation study. *Int. J. Radiat. Oncol. Biol.*, 69(4), pp. 1100-1109.
- 38 Holm, S., 1979. A simple sequentially rejective multiple test procedure. *Scandinavian Journal of Statistics*, 6(2), pp.
39 65-70.

- 1 ICRU Report 62, 1999. *Prescribing, recording and reporting photon beam therapy (supplement to ICRU report 50)*.
2 Bethesda, USA.
- 3 Jamema SV, Mahantshetty U, Andersen E, Noe KØ, Sørensen TS, Kallehauge JF, Shrivastava SK, Deshpande DD,
4 Tanderup K , 2015. Uncertainties of deformable image registration for dose accumulation of high-dose regions in
5 bladder and rectum in locally advanced cervical cancer. *Brachytherapy* 14(6), pp. 953-62.
- 6 Konishi, K., Yoshioka, Y., Isohashi, F. & Sumida, I., 2009. Correlation between dosimetric parameters and late
7 rectal and urinary toxicities in patients treated with high-dose-rate brachytherapy used as monotherapy for prostate
8 cancer. *Int. J. Radiat. Oncol. Biol.*, 75(4), pp. 1003-1007.
- 9 Lang, S., Kirisits, C., Dimopoulos, J. & Georg, D., 2007. Treatment Planning for MRI Assisted Brachytherapy of
10 Gynecologic Malignancies Based on Total Dose Constraints. *Int. J. Radiat. Oncol.*, 69(2), pp. 619-627.
- 11 Ling, C. et al., 1987. CT-assisted assessment of bladder and rectum dose in gynecological implants. *Int. J. Radiat.*
12 *Oncol. Biol. Phys.*, 13(10), pp. 1577-1582.
- 13 Mazon, R., Maroun, P. & Castelnaud-Marchand, P., 2015. Pulsed-dose rate image-guided adaptive brachytherapy
14 in cervical cancer: Dose-volume effect relationships for the rectum and bladder. *Radiotherapy and oncology*, 116(2),
15 p. 116:226.
- 16 Miller, R., 1981. *Simultaneous Statistical Inference*. 2nd ed. New York: Springer Verlag.
- 17 Myronenko, A. & Song, X., 2010. Point-Set Registration: Coherent Point Drift. *IEEE Trans. Pattern Anal.*, 32(12),
18 pp. 2262-2275.
- 19 Nag, S., 2006. Controversies and new developments in gynecologic brachytherapy: Image-based intracavitary
20 brachytherapy for cervical carcinoma. *Sem. Rad. Onc.*, 16(3), pp. 164-167.
- 21 Nag, S. et al., 2004. Proposed guidelines for image-based intracavitary brachytherapy for cervical carcinoma: report
22 from Image-Guided Brachytherapy Working Group. *Int. J. Radiat. Oncol. Biol. Phys.*, 60(4), pp. 1160-72.
- 23 Nilsson, S., Norlén, B. & Widmark, A., 2004. A systematic overview of radiation therapy effects in prostate cancer.
24 *Acta. Oncol.*, 43(4), pp. 316-381.
- 25 Noe, K., Tanderup, K. & Sorensen, T., 2011. Surface membrane based bladder registration for evaluation of
26 accumulated dose during brachytherapy in cervical cancer. *IEEE Int. Sym. on Biomedical Imaging: From Nano to*
27 *Macro*, pp. 1253-1256.
- 28 Patra, N., Manir, K., Basu, S. & Goswami, J., 2013. Effect of bladder distension on dosimetry of organs at risk in
29 computer tomography based planning of high-dose-rate intracavitary brachytherapy for cervical cancer. *J. Contemp.*
30 *Brachytherapy*, 5(1), pp. 3-9.
- 31 Pavamani, S. et al., 2011. Image-guided brachytherapy for cervical cancer: a Canadian Brachytherapy Group survey.
32 *Brachytherapy*, 10(5), pp. 345-351.
- 33 Rubin, P., Constine, L. S., Fajardo, L. F. & Phillips, T. L., 1995. Overview of late effects normal tissues (LENT)
34 scoring system. *Radiother. Oncol.*, Volume 35, pp. 9-10.
- 35 Pötter, R., Haie-Meder, C. & Limbergen, E. V., 2006. Recommendations from Gynaecological (GYN) GEC ESTRO
36 Working Group (II): concepts and terms in 3D image based treatment planning in cervix cancer brachytherapy:
37 aspects of 3D imaging, radiation physics, radiobiology, and 3D dose volume parameters. *Radiother. Oncol.*, 78(1),
38 pp. 67-77.
- 39 Powell, M. E., 2010. Modern Radiotherapy and Cervical Cancer. *Int. J. Gynecol. Cancer*, 20(S2), pp. S49-S51.

- 1 Rosewall, T., Catton, C., Currie, G. & Bayley, A., 2010. The relationship between external beam radiotherapy dose
2 and chronic urinary dysfunction—a methodological critique. *Radiother. Oncol.*, 97(1), pp. 40-47.
- 3 Routledge, J., Burns, M., Swindell, R. & Khoo, V., 2003. Evaluation of the LENT-SOMA scales for the prospective
4 assessment of treatment morbidity in cervical carcinoma. *Int. J. Radiat. Oncol.*, 56(2), pp. 502-510.
- 5 Sabater, S., Andres, I., Sevillano, M. & Berenguer, R., 2014. Dose accumulation during vaginal cuff brachytherapy
6 based on rigid/deformable registration vs. single plan addition. *Brachytherapy*, 13(4), pp. 343-351.
- 7 Tamhane, A., 1996. Multiple comparisons. *Handbook of Statistics*, Volume 13, pp. 587-630.
- 8 Tanderup, K. et al., 2010. Adaptive management of cervical cancer radiotherapy. *Semin. Radiat. Oncol.*, 20(2), pp.
9 121-129.
- 10 Teo, B., Millar, L., Ding, X. & Lin, L., 2015. Assessment of cumulative external beam and intracavitary
11 brachytherapy organ doses in gynecologic cancers using deformable dose summation. *Radiother. Oncol.*, 115(2), pp.
12 195-202.
- 13 Whitley, A., Dragovic, A., Shen, S. & Wu, S., 2013. Effects of Full Versus Empty Bladder on Total Equivalent
14 Dose to Organs at Risk in 3D Image-Based Planning of High-Dose-Rate Intracavitary Brachytherapy for Cervical
15 Cancer. *Int. J. Radiat. Oncol. Biol. Phys.*, 87(2), p. Supplement 1 S404.
- 16 Wiebe, E. M., Surry, K. & D'Souza, D. P., 2010. Rectal and Bladder Toxicity in Patients Receiving CT-guided
17 HDR Interstitial Brachytherapy for Gynecologic Malignancies. *Int. J. Radiat. Oncol. Biol.*, 78(3), pp. Supplement, 1
18 S422.
- 19 Wognum, S., Heethuis, S. & Rosario, T., 2014. Validation of deformable image registration algorithms on CT
20 images of ex vivo porcine bladders with fiducial markers. *Med. Phys.*, 41(7), p. 071916.
- 21 Xiong, L., Viswanathan, A., Stewart, A. & Haker, S., 2006. Deformable structure registration of bladder through
22 surface mapping. *Med. Phys.*, 33(6), pp. 1848-1856.
- 23 Yamashita, H., Nakagawa, K., Okuma, K. & Sakumi, A., 2012. Correlation Between Bladder Volume and Irradiated
24 Dose of Small Bowel in CT-based Planning of Intracavitary Brachytherapy for Cervical Cancer. *Jpn. J. Clin.
25 Oncol.*, 42(4), pp. 302-308.
- 26 Yan, D., Jaffray, D. & Wong, J., 1999. A model to accumulate fractionated dose in a deforming organ. *Int. J. Radiat.
27 Oncol. Biol.*, 44(3), pp. 665-675.
- 28 Zakariaee, R., Hamarneh, G., Brown, C. & Spadinger, a. I., 2016. Validation of non-rigid point-set registration
29 methods using a porcine bladder pelvic phantom. *Phys. Med. Biol.*, 61(2), pp. 825-54.